Characterization of magnetron-sputtered partially ionized aluminum deposition

D. B. Hayden, D. R. Juliano, K. M. Green, D. N. Ruzic, C. A. Weiss et al.

Citation: J. Vac. Sci. Technol. A **16**, 624 (1998); doi: 10.1116/1.581078

View online: http://dx.doi.org/10.1116/1.581078

View Table of Contents: http://avspublications.org/resource/1/JVTAD6/v16/i2

Published by the AVS: Science & Technology of Materials, Interfaces, and Processing

Related Articles

Low-temperature Al–Ge bonding for 3D integration
J. Vac. Sci. Technol. B 30, 06FK01 (2012)

Die singulation technologies for advanced packaging: A critical review
J. Vac. Sci. Technol. B 30, 040801 (2012)

Monolithic integration of silicon CMOS and GaN transistors in a current mirror circuit
J. Vac. Sci. Technol. B 30, 02B101 (2012)

Multilayer infrared metamaterial fabrication using membrane projection lithography
J. Vac. Sci. Technol. B 29, 06FF04 (2011)

Surface activated bonding of copper through silicon vias and gold stud bumps at room temperature
J. Vac. Sci. Technol. A 29, 021007 (2011)

Additional information on J. Vac. Sci. Technol. A

Journal Homepage: http://avspublications.org/jvsta

Journal Information: http://avspublications.org/jvsta/about/about_the_journal

Top downloads: http://avspublications.org/jvsta/top_20_most_downloaded

Information for Authors: http://avspublications.org/jvsta/authors/information_for_contributors

ADVERTISEMENT

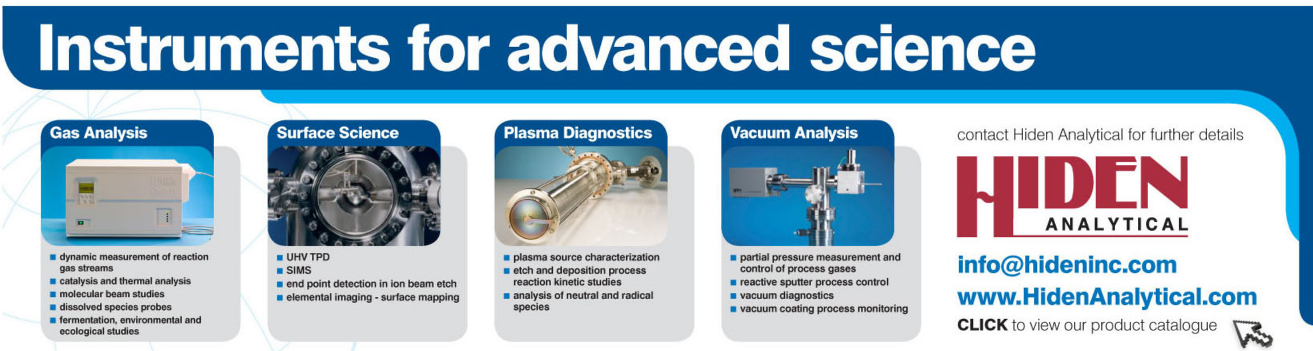

Downloaded 25 Dec 2012 to 192.17.144.42. Redistribution subject to AVS license or copyright; see http://avspublications.org/jvsta/about/rights_and_permissions

Characterization of magnetron-sputtered partially ionized aluminum deposition

D. B. Hayden,[a] D. R. Juliano, K. M. Green, and D. N. Ruzic
University of Illinois, Urbana, Illinois 61801

C. A. Weiss,[b] K. A. Ashtiani, and T. J. Licata
Materials Research Corporation, Orangeburg, New York 10962

(Received 7 July 1997; accepted 21 November 1997)

A rotating magnet dc planar magnetron with a 33-cm diameter aluminum target is coupled with a secondary plasma source to ionize the sputtered metal neutral flux to control the angular distribution of the flux arriving at the surface of the substrate. For this purpose, a radio-frequency (rf) plasma is created between the sputtering target and substrate by a three-turn coil located in the vacuum chamber. The rf plasma increases the electron temperature and density, which results in significant ionization of the neutral metal flux from the sputtering target. By applying a small negative bias to the substrate, metal ions are drawn to the substrate at normal incidence. A gridded energy analyzer and a quartz crystal microbalance (QCM) were used to determine the ion and neutral deposition rates. From this, the ionization fraction of the flux incident onto the QCM is determined. © *1998 American Vacuum Society.* [S0734-2101(98)02602-5]

I. INTRODUCTION

The dc magnetron sputtering is used extensively to deposit films that serve as interconnects in integrated circuits (ICs). In this physical vapor deposition (PVD) process, metal atoms are sputtered from a dc-biased target with ejection energies of a few eV.[1] The angular distribution of the ejected atoms is roughly a cosine distribution, and is further broadened by gas phase scattering, yielding insufficient bottom coverage and voids during filling of high aspect ratio (>1) features.[2] As device geometries are reduced to sub-0.35 μm and contact and via aspect ratios increase to >3, semiconductor IC manufacturers are looking for alternatives to physical collimation techniques[3] and chemical vapor deposition technologies.[4] The problems associated with conventional sputtering sources can be overcome by ionizing the metal flux and applying a bias on the substrate to accelerate the metal ions through the plasma sheath to the substrate surface. Since the sheath thickness is smaller than the mean free path and the electric field in the sheath is normal to the substrate, a narrow angular distribution is achieved. Ionized PVD enables the electrostatic collimation of materials for IC applications without the inherent problems of physical collimators (e.g., lower deposition rates, collimator clogging, uniformity changes, particulate formation, poor bottom-corner step coverage, and high effective cost[5]).

Ionized PVD has been demonstrated by introducing an inductively coupled plasma (ICP) coil between the substrate and target.[6–8] Applying rf power (typically at 13.56 MHz) to the coil increases the electron temperature and density. The net result is an increase in the ionization rate of the metal atoms with a corresponding increase in the ionization fraction of the flux to the substrate.

In this article we demonstrate ionized PVD and report on the plasma properties as measured by a quartz crystal microbalance (QCM), a gridded energy analyzer (GEA), and Langmuir probes. Conventional PVD operation is at 1–5 mTorr, with metal ionization percentages in the single digits. This low ionization is due to decreased electron density, less effective Penning ionization, and nearly collisionless transport of aluminum at low argon pressures.[9] The operation pressure range with the ICP coil for ionized PVD is 15–35 mTorr, and the ionization fraction of the metal flux that reaches the bottom of an $\sim 1:1$ aspect ratio via is over 80%.

II. EXPERIMENT

The sputtering tool used is a rotating magnet dc planar magnetron with a 33-cm diameter aluminum target. The chamber is cryopumped and has a base pressure of 7.0×10^{-8} Torr. A cross section of the chamber geometry, the diagnostic components, and the ICP coil are shown in Fig. 1. A three-turn aluminum water-cooled coil powered by a 1.5 kW rf (13.56 MHz) power supply matched with a variable input capacitor (600–1200 pF) and end-of-coil grounding capacitor (600–800 pF) is used.

The diagnostic, described in detail elsewhere,[10] is used to measure the ionization fraction and the deposition rate of the metal flux, and consists of a QCM embedded under a three-grid GEA shown in Fig. 2. The term ''ionization fraction'' is used to describe the fraction of the metal flux reaching the bottom of the diagnostic. Similar embodiments of this diagnostic have been previously discussed for helicon and ECR etching,[11–13] and in ionized PVD[7,14] applications. Complementary measurements were also obtained using a Langmuir probe to determine the electron temperature and density at different pressures and different magnetron powers. These data are shown in Table I and the time-resolved probe techniques are outlined in Refs. 15 and 16 for rf plasmas.

The deposition rate is monitored by the QCM and is calibrated with film thickness profilometer measurements on glass substrates. This is necessary to account for the trans-

[a]Electronic mail: doug@starfire.ne.uiuc.edu
[b]Electronic mail: appliedtechnologies@compuserve.com

Downloaded 25 Dec 2012 to 192.17.144.42. Redistribution subject to AVS license or copyright; see http://avspublications.org/jvsta/about/rights_and_permissions

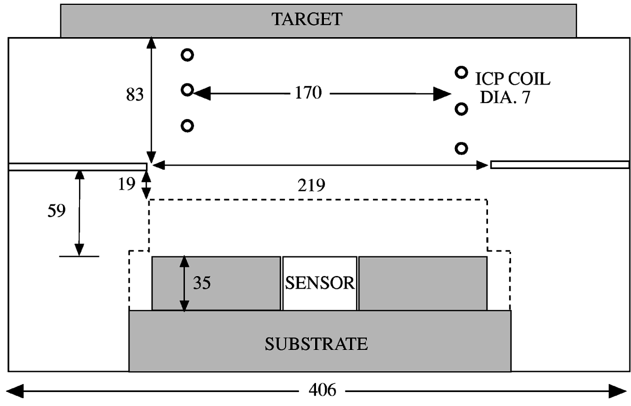

FIG. 1. A cross-section schematic of the sputtering chamber. The dotted outline shows the location of the substrate in its raised position. The sensor contains the gridded energy analyzer and quartz crystal microbalance, as seen in Fig. 2.

parency of the grids and the difference in the vertical position of the substrate plane and the QCM.

The ionization fraction is calculated from the total (ion and neutral) and neutral deposition rates, thus two measurements with distinct grid settings are required. To measure the aluminum total deposition, all three grids are biased at −30 V. The substrate is also biased at −30 V. To measure the aluminum neutral deposition the retarding grid is set at 30 V (above the plasma potential of 10–15 V). This consistently screened out the vast majority of the ions. The ionization fraction is the difference between the total and neutral deposition rates divided by the total deposition rate.

In operations, the plasma goes through a transition from capacitively coupled to inductively coupled. At high pressures (>25 mTorr) this is observed by a sharp increase in glow intensity as expected.[17] Below 25 mTorr the change is not as abrupt, but a gradual increase in intensity is noted. At all pressures the transition to the inductively coupled mode is noticeable by observing the reflected power on the rf supply.

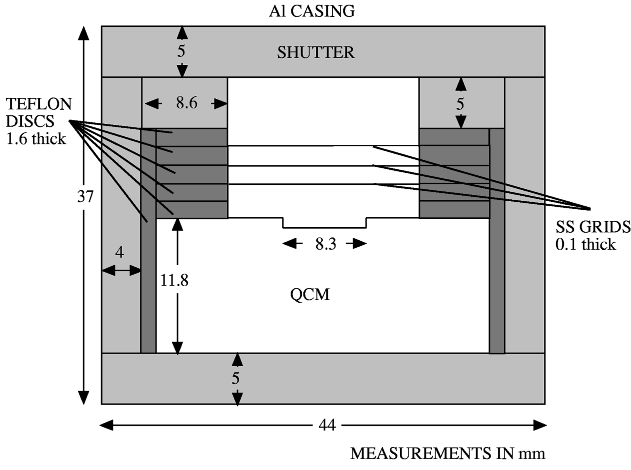

FIG. 2. A cross-section schematic of the gridded energy analyzer and quartz crystal microbalance diagnostic.

TABLE I. Langmuir probe electron temperature and density measurements at varying magnetron powers and pressures (all at 800 W ICP power).

Pressure (mTorr)	Magnetron power (kW)	T_e (eV)	n_e (cm^{-3})
25	2.0	2.7±0.5	$2.6\pm0.3\times10^{11}$
	2.5	2.9±0.3	$2.4\pm0.2\times10^{11}$
	3.0	2.1±0.2	$2.1\pm0.2\times10^{11}$
35	2.0	2.6±0.5	$3.1\pm0.3\times10^{11}$
	2.5	1.8±0.2	$3.2\pm0.3\times10^{11}$

In the capacitive mode the forward and reflected power both increase as the rf power is increased, but as the transition to inductive mode begins, the reflected power drops as the forward power is further increased. This continues until the power supply current peaks, usually around a power of 1200 W. The efficiency of the coupling is much higher when in the inductive mode. It should be noted that there will always be some capacitive coupling to the plasma from grounded chamber walls. The term inductive mode is used to imply that most of the rf power is input to the system inductively, but by no means to all of the power.

Data are taken with the target-to-substrate throw distance at 10.2 cm and at 14.2 cm. The substrate is raised to see the effect of different throw distances on the deposition rate and ionization fraction. Langmuir probe data are only available with the lowered substrate. The dotted outline in Fig. 1 shows the location of the substrate and diagnostics in the raised position.

The ionization fraction that reaches flat portions of the substrate is smaller than that which reaches the QCM since neutral atoms that hit the inside walls of the diagnostic are part of the flux in the substrate plane. This geometric effect and the calibration is discussed in Ref. 10. Note that the ionization fractions at the bottom of a cylindrical via would be the same as those measured here if the via had the same aspect ratio as our diagnostic (1.8:1) since the geometric effect would be the same.

III. RESULTS AND DISCUSSION

Figure 3 shows the deposition rate and ionization fraction at three different magnetron powers (2.0, 2.5, and 3.0 kW) and three different pressures (15, 25, and 35 mTorr) for the lowered target-to-substrate distance of 14.2 cm. The rf power is held constant at 800 W. As one would expect, higher magnetron power leads to a higher deposition rate because more neutral atoms are sputtered from the magnetron into the plasma. Higher pressures lead to a lower deposition rate because more atoms are scattered to the walls of the chamber. A competing effect of pressure is seen from the ionization fraction data. The increased scattering at higher pressures leads to a higher ionization fraction since the residence time of a sputtered atom in the rf plasma is longer.

Figure 4 again shows the deposition rate and ionization fraction as a function of power and pressure for the raised target-to-substrate distance of 10.2 cm. The effects of pres-

Downloaded 25 Dec 2012 to 192.17.144.42. Redistribution subject to AVS license or copyright; see http://avspublications.org/jvsta/about/rights_and_permissions

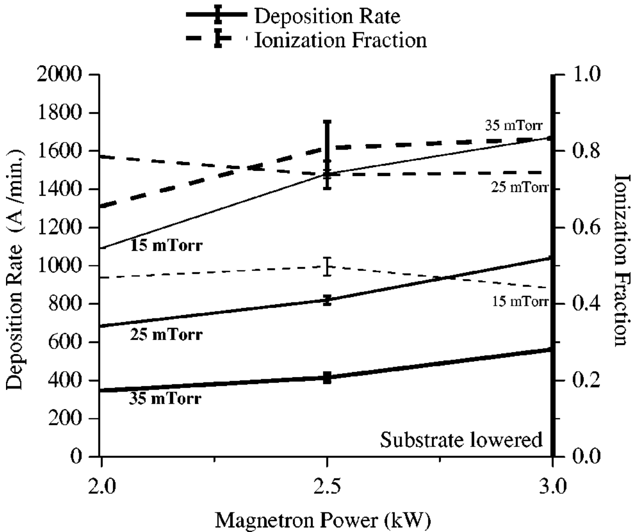

FIG. 3. Deposition rate and ionization fraction vs magnetron power for 800 W ICP power at different pressures with substrate in lowered position. Representative error bars are shown. The large error in the ionization fraction at 35 mTorr is due to a low deposition rate when the ions are screened out.

sure are identical, except a slightly lower or equal deposition rate is actually seen for the highest power (3.0 kW) at the higher pressures of 25 and 35 mTorr.

Figures 5 and 6 explain this phenomenon. In Fig. 5 the deposition rate due to neutral atoms is only shown for both substrate positions and all three pressures and powers. It behaves in a very understandable fashion. Lower pressure, higher power, and a shorter target-to-substrate distance leads to more neutral deposition. Figure 6 shows the deposition rate due only to ions for both substrate positions and all three pressures and powers. At the lower substrate position the ion deposition rate mimics that of the neutrals-lower pressure and higher power lead to more ion deposition. There is a sufficient ionization volume of plasma when the substrate is

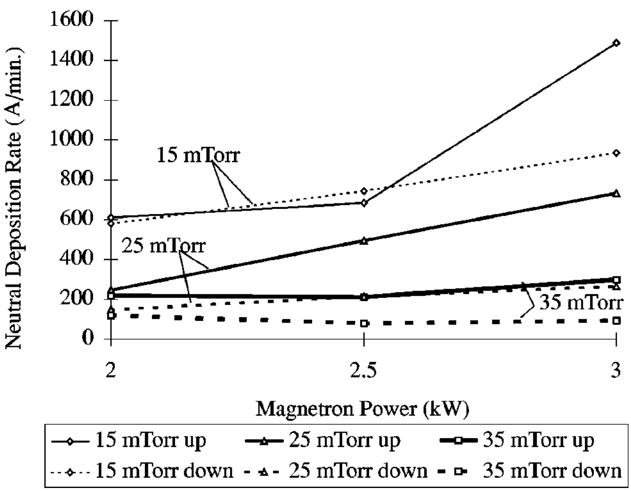

FIG. 5. Neutral deposition rate vs magnetron power for 800 W ICP power at different substrate heights. Error bars are shown for every point.

lowered such that the number of particles becoming ionized is driven by the source term of the sputtered particles.

When the substrate is raised, Fig. 6 shows that the ion deposition rate is higher at higher pressures. A longer neutral residence time in the rf plasma becomes the dominant effect on the ionization. With the target and substrate close, many fewer particles are actually scattered to the walls. The effect of magnetron power on the deposition rate of ions generally increases the source term and the rates increase. At the highest power however, such an overwhelming flux of metal is added to the plasma that it cools. This is supported by Langmuir probe data showing the electron temperature drop at the higher magnetron powers (Table I). Therefore the ion deposition rates are lower for all three pressures at the highest power even though the neutral atom deposition rate increases. This explains the drop in ionization fraction seen in Fig. 4.

The ion deposition at 15 mTorr does not increase with a shorter target-to-substrate distance as shown in Fig. 6 like it

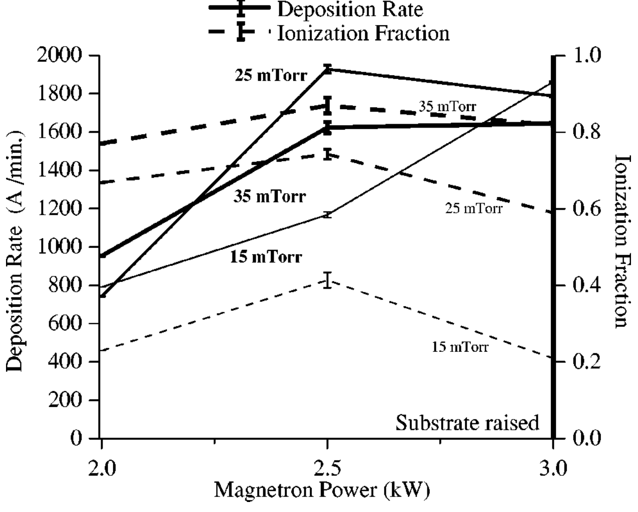

FIG. 4. Deposition rate and ionization fraction vs magnetron power for 800 W ICP power at different pressures with the substrate in raised position. Representative error bars are shown.

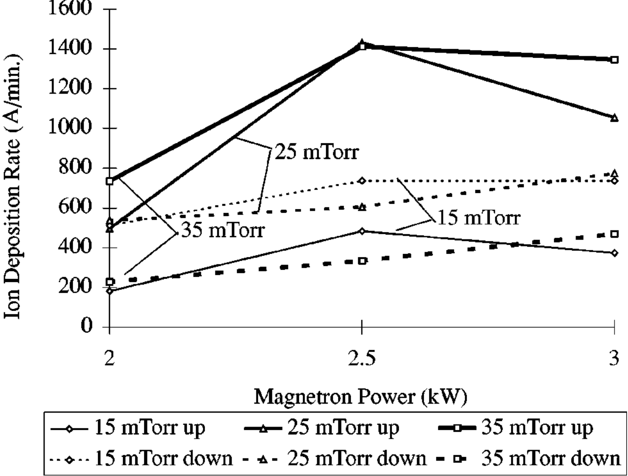

FIG. 6. Ion deposition rate vs magnetron power for 800 W ICP power at different substrate heights. Error bars are shown for every point.

Downloaded 25 Dec 2012 to 192.17.144.42. Redistribution subject to AVS license or copyright; see http://avspublications.org/jvsta/about/rights_and_permissions

does at 25 and 35 mTorr. This is due to two competing effects. The first effect is the scattering, which decreases deposition at larger target-to-substrate distances. The second effect is the increased neutral residence time at larger target-to-substrate distances, which increases the number of ions. At 15 mTorr the deposition is closer to a line-of-sight process than at higher pressures, thus the scattering effect is reduced and the sum of the two effects is to increase the ion deposition at larger target-to-substrate distances. This is supported by ionization fractions between 45% and 50% for the lowered substrate versus between 20% and 40% for the raised substrate at 15 mTorr (Figs. 3 and 4).

The added ICP coil provides a good source of additional plasma, raising the electron temperature and density which leads to increased ionization of the sputtered metal flux. This may provide the directional flux needed to fill high aspect ratio trenches and vias for the next generation of computer chips.

ACKNOWLEDGMENTS

This project was primarily funded by the Materials Research Corporation. In addition, K. M. Green was supported by the Nuclear Engineering/ Health Physics Fellowship Program administered by Oak Ridge Institute for Science and Education for the U. S. Department of Energy. D. R. Juliano was supported by a Fannie and John Hertz Foundation Fellowship. Special thanks goes out to Martin Neumann and Eric Skarpac for aiding with the data collection and figures.

[1] D. N. Ruzic, in *Handbook of Plasma Processing Technology,* edited by S. M. Rossnagel, J. J. Cuomo, and W. D. Westwood (Noyes, Park Ridge, NJ, 1990), p. 86.
[2] S. M. Rossnagel, Thin Solid Films **263**, 1 (1995).
[3] S. M. Rossnagel, D. Mikalsen, H. Kinoshita, and J. J. Cuomo, J. Vac. Sci. Technol. A **9**, 261 (1991).
[4] G. L. Lucovsky, D. V. Tsu, and R. J. Markunas, in *Handbook of Plasma Processing Technology,* edited by S. M. Rossnagel, J. J. Cuomo, and W. D. Westwood (Noyes, Park Ridge, NJ, 1990), p. 387.
[5] S. M. Rossnagel, Semicond. Int., 99 (1996).
[6] M. Yamashita, J. Vac. Sci. Technol. A **7**, 151 (1989).
[7] S. M. Rossnagel and J. Hopwood, J. Vac. Sci. Technol. B **12**, 449 (1994).
[8] P. F. Cheng, S. M. Rossnagel, and D. N. Ruzic, J. Vac. Sci. Technol. B **13**, 203 (1995).
[9] J. Hopwood and F. Qian, J. Appl. Phys. **78**, 758 (1995).
[10] K. M. Green, D. B. Hayden, D. R. Juliano, and D. N. Ruzic, Rev. Sci. Instrum. **68**, 4555 (1997).
[11] A. G. Perry, D. Vender, and R. W. Boswell, J. Vac. Sci. Technol. B **9**, 310 (1991).
[12] M. Matsuoka and K. Ono, Appl. Phys. Lett. **50**, 1864 (1987).
[13] M. Matsuoka and K. Ono, J. Vac. Sci. Technol. A **6**, 25 (1988).
[14] S. M. Rossnagel and J. Hopwood, Appl. Phys. Lett. **63**, 3285 (1993).
[15] R. B. Turkot and D. N. Ruzic, J. Appl. Phys. **73**, 2173 (1993).
[16] D. N. Ruzic, *Electric Probes for Low Temperature Plasmas* (AVS Monograph Series, New York, 1994).
[17] J. Hopwood, Plasma Sources Sci. Technol. **1**, 109 (1992).

Downloaded 25 Dec 2012 to 192.17.144.42. Redistribution subject to AVS license or copyright; see http://avspublications.org/jvsta/about/rights_and_permissions